LOW ENERGY HADRON PHYSICS WITH carlomat_3.0*

Karol Kołodziej

Institute of Physics, University of Silesia
Uniwersytecka 4, 40-007 Katowice, Poland
karol.kolodziej@us.edu.pl

(Received October 16, 2015)

carlomat_3.0, a new version of the metaprogram for generating codes for Monte Carlo calculations of the leading order cross sections and simulations of multiparticle reactions, is dedicated to the description of the processes $e^+e^- \to$ hadrons at low center-of-mass energies in the framework of effective models, such as the Resonance Chiral Theory and the Hidden Local Symmetry model, or the model of the electromagnetic interaction of nucleons. The program offers a number of new options which give the user a better control over the effective models implemented.

DOI:10.5506/APhysPolB.46.2267
PACS numbers: 02.70.–c, 02.70.Uu, 14.65.Ha

1. Motivation

The knowledge of the energy dependence of the cross section of e^+e^- annihilation into hadrons, $\sigma_{e^+e^-\to\text{hadrons}}(s)$, allows to determine, through dispersion relations, hadronic contributions to the vacuum polarization. Better precision of the latter is important to improve precision of theoretical predictions for the muon anomaly and evolution of the fine structure constant from the Thomson limit to high energy scales, which would be of particular relevance in the analyses of data from the future e^+e^- collider, where $\sim 10^{13} Z$s are expected to be produced in a period of a few years, see *e.g.*, presentations by Riemann [1], Lesiak [2] and Riemann [3] at this conference.

At low centre-of-mass energies, below the J/ψ threshold, $\sigma_{e^+e^-\to\text{hadrons}}(s)$ must be measured, either by the initial beam energy scan or with the use of a radiative return method, and compared with predictions of a Monte Carlo (MC) program. To reach the desired precision level of such comparison for the dominant hadronic channels, radiative corrections must be included

* Presented at the XXXIX International Conference of Theoretical Physics, "Matter to the Deepest", Ustroń, Poland, September 13–18, 2015.

in the predictions. However, for many final states where the experimental accuracy is not high, it is enough to have the leading order (LO) predictions.

The most promising theoretical framework for the description of $e^+e^- \to$ hadrons at low energies is the Resonance Chiral Theory (RχT) [4] or the Hidden Local Symmetry (HLS) model [5] which, among others, involve the photon–vector meson mixing and a number of vertices of a rather complicated Lorentz tensor structure. Already at low energies, the hadronic final states may consist of several particles, such as pions, kaons or nucleons, which can be accompanied by one or more photons or light fermion pairs, such as e^+e^- or $\mu^+\mu^-$. The number of Feynman diagrams of such multi-particle reactions grows substantially with increasing number of interaction vertices and mixing terms of the effective models. Therefore, it is highly desirable to automatize the calculations.

To achieve this goal, program `carlomat` [6, 7] has been substantially modified in order to incorporate a photon–vector meson mixing and include the Feynman interaction vertices of RχT or the HLS model, which were provided by Jegerlehner [8], and vertices of the effective Lagrangian of the electromagnetic (EM) interaction of nucleons. A new version of the program, `carlomat_3.0` [9], allows to generate automatically the MC programs dedicated to the description of processes $e^+e^- \to$ hadrons at low centre-of-mass energies.

2. New Feynman rules in the program

In spite of being conceptually quite simple, the implementation of particle mixing required substantial changes in the code generation part of the program. This is because of the fact that the topologies of Feynman diagrams are in `carlomat` generated for models with triple and quartic couplings, *i.e.*, there are no couplings between two particles, as actually is the mixing term depicted in Fig. 1.

$$\equiv \quad -e f_{\gamma V}(q^2)\, g^{\mu\nu},$$

Fig. 1. The photon–vector meson mixing γ–V, with $V = \rho^0, \omega, \phi$, $\rho_1 = \rho(1450)$, $\rho_2 = \rho(1700)$.

Therefore, the particle mixing must be added at the stage of the program in which the diagram topologies are checked against the Feynman rules. While doing so, two (three) particles are combined into the third (fourth) leg of a triple (quartic) interaction vertex which is then folded with the adjacent

Feynman propagator to form an off-shell particle. The latter is represented by an array of spinors, polarization vectors or scalars, with elements labelled with the polarization indices of spinors or polarization vectors of which it is formed. To facilitate the comparison, each topology is divided into two parts, each being checked against the Feynman rules separately. If the particle mixing is present, the program checks whether the propagator of the off-shell particle can be mixed or not, if so, a new off-shell particle is formed.

To exemplify this procedure, let us consider the process

$$e^+(p_1)\, e^-(p_2) \;\to\; \pi^+(p_3)\, \pi^-(p_4)\, \mu^+(p_5)\, \mu^-(p_6)\, \gamma(p_7)\,, \tag{1}$$

two Feynman diagrams of which, both containing the γ–ρ^0 mixing of Fig. 1, are depicted in Fig. 2. The particle four-momenta of process (1) are indicated in parentheses.

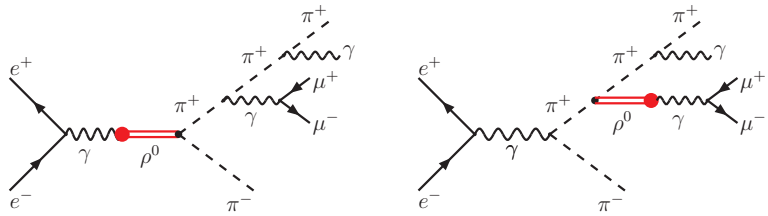

Fig. 2. Feynman diagrams of $e^+e^- \to \pi^+\pi^-\mu^+\mu^-\gamma$ with γ–ρ^0 mixing.

Using the Feynman rules listed in Ref. [9] their amplitudes can be written in terms of the polarization four-vectors:

$$\varepsilon^{\mu}_{12} = i\frac{-g^{\mu\nu}}{s}\,\bar{v}(p_1)(-ie\gamma_\nu)u(p_2)\,, \quad \varepsilon^{\mu}_{56} = i\frac{-g^{\mu\nu}}{p^2_{56}}\,\bar{u}(p_6)(-ie\gamma_\nu)v(p_5)\,, \tag{2}$$

$$\varepsilon^{\mu}_{56\,\mathrm{mix}} = i\frac{-g^{\mu\nu} + \frac{p^{\mu}_{56}p^{\nu}_{56}}{M^2\left(p^2_{56}\right)}}{p^2_{56} - M^2\left(p^2_{56}\right)}(-e)f_{\gamma\rho^0}\left(p^2_{56}\right)\varepsilon_{56\,\nu} \tag{3}$$

and scalars:

$$s_{37} = \frac{i}{p^2_{37} - m^2_{\pi}}\, ief_{\gamma\pi^+\pi^-}\left(p^2_7\right)(2p_3 + p_7)_{\mu}\varepsilon^{\mu}(p_7)\,, \tag{4}$$

$$s_{3756} = \frac{i}{p^2_{56} - m^2_{\pi}}\, s_{37} ief_{\gamma\pi^+\pi^-}\left(p^2_{56}\right)(2p_{37} + p_{56})_{\mu}\varepsilon^{\mu}_{56}\,, \tag{5}$$

$$s_{124} = \frac{i}{(p_{12} - p_4)^2 - m^2_{\pi}}\, if_{\rho^0\pi^+\pi^-}(s)(p_{12} - 2p_4)_{\mu}\varepsilon^{\mu}_{12} \tag{6}$$

in the following form

$$M_a = \varepsilon_{12\,\mu}(-e) f_{\gamma\rho^0}(s)\, i \frac{-g^{\mu\nu} + \frac{p_{12}^{\mu} p_{12}^{\nu}}{M^2\left(p_{12}^2\right)}}{s - M^2\left(p_{12}^2\right)} i f_{\rho^0\pi^+\pi^-}(s)(p_{12} - 2p_4)_{\nu} s_{3756}\,, \quad (7)$$

$$M_b = s_{124} i f_{\rho^0\pi^+\pi^-}\left(p_{56}^2\right)(2p_{37} + p_{56})_{\mu} \varepsilon_{56\,\mathrm{mix}}^{\mu} s_{37}\,. \quad (8)$$

In Eqs. (2)–(8), particle polarization indices have been suppressed and the following notation has been used: $p_{12} = p_1 + p_2$, $p_{37} = p_3 + p_7$, $p_{56} = p_5 + p_6$, $s = p_{12}^2$ and $M^2(q^2) = m_\rho^2 - i m_\rho \Gamma_\rho(q^2)$, with $\Gamma_\rho(q^2)$ being the running ρ-meson width, which is introduced in order to avoid poles in the LO ρ-meson propagator.

The mixing term of Fig. 1 introduces an extra power of e and it should be included at most once in a Feynman diagram. Therefore, the particle with mixing, such as that represented by the polarization four vector $\varepsilon_{56\,\mathrm{mix}}^{\mu}$ of Eq. (3), must be appropriately tagged in order not to be mixed again. The diagram with mixing can be obtained either by joining a particle with mixing with a particle without mixing, or by joining two unmixed particles with one of the mixing terms of Fig. 1.

The modifications of the code generation part of the program that were necessary in order to include calls to subroutines for computation of the Feynman interaction vertices of the RχT and the HLS model, and the effective Lagrangian of the electromagnetic interaction of spin 1/2 nucleons were more straightforward. Obviously, a number of new subroutines had to be written to compute the helicity amplitudes involving the mixing terms and the interaction vertices of new Lorentz tensor structures. Moreover, an interface to a subroutine for computation of the EM form factors of nucleons, adopted from `PHOKARA` [10], was written.

3. New program options

A number of new options were introduced in the program to enable a better control over the effective models implemented. Some of them are described below.

To give a better control over the mixing contributions to a given process, subroutines for computation of the helicity amplitudes of building blocks or complete Feynman diagrams involving mixing are equipped with the option:

`iwgt=0/1,2,...` if the additional complex factor $c_1, c_2, \ldots$ `is not/is` to be included in $f_{\gamma V}(q^2)$.

The complex factor c_j, $j = 1, 2, \ldots$ is given by $c_j = w_j\, e^{i\varphi_j} f_j(q^2)$, where w_j is a positive weight, φ_j is an angle in degrees, which should be both specified for each possible particle mixing term in the main program for the MC computation, and $f_j(q^2)$ is a possible additional four-momentum transfer

dependence. Only three simple dependencies corresponding to `iwgt=1,2,3` are currently defined in the program, but the user can easily add more options by implementing new `else if(iwgt == ...) then` conditions in subroutine `weightfactor`.

All subroutines that are used to compute the building blocks or the complete helicity amplitudes of the Feynman diagrams containing vertices of the implemented effective model have been supplied with the *running coupling option*. The actual form of the running coupling must be defined by the user in subroutine `runcoupl`. However, the four-momentum transfer q is determined automatically from the four-momentum conservation in the corresponding interaction vertex at the stage of a code generation. Many couplings of the RχT and the HLS model are not known well enough and must be adjusted in consecutive runs of the program in order to obtain satisfactory description of the experimental data. If there are no hints as to the form of the running couplings, then it is recommended to set the corresponding running coupling option to 0, which means that the fixed coupling is to be used in the computation.

The subroutines for computation of the four vectors representing vector mesons have been, in addition, supplied with the *running width option*:

`iwdth_name=0/1,2,3` if the `fixed/running` width of the vector particle should be used,

where choices $1, 2, 3$ refer to different running width options, which again can easily be extended by the user. The actual names of the option: `igmrh, igmom,igmph,igmr1,igmr2` for the $\rho^0, \omega, \phi, \rho_1, \rho_2$ mesons, respectively, are created automatically at the stage of a code generation.

An important new option in the program that allows to test the EM gauge invariance for processes with one ore more external photons is

`igauge=1,2,.../else` if the gauge invariance `is/is not` to be tested,

where $1, 2, \ldots$ is the number of a photon in the considered process, counting from left to right, the polarization four-vector of which is replaced with its four-momentum.

To illustrate how the EM gauge invariant tests work in practise, the cross sections of two radiative processes: $e^+e^- \to \pi^+\pi^-\pi^+\pi^-\gamma$ and process (1) at three centre-of-mass energies, with the following cuts:

$$\theta_{\gamma\, l} > 5^\circ, \qquad \theta_{\gamma\, \pi} > 5^\circ, \qquad E_\gamma > 10 \text{ MeV} \tag{9}$$

are given in Table I. Both cross sections drop by about 32 orders of magnitude if `igauge=1`, *i.e.*, the EM gauge invariance test is satisfied perfectly well. The inclusion of some vertices, as it was exemplified in Ref. [9], or the q^2-dependent particle widths may spoil the EM gauge invariance.

TABLE I

Cross sections in pb of two radiative processes with cuts (9). The numbers in parentheses show the MC uncertainty of the last decimal.

$\sqrt{s}$	$e^+e^- \to \pi^+\pi^-\pi^+\pi^-\gamma$		$e^+e^- \to \pi^+\pi^-\mu^+\mu^-\gamma$	
[GeV]	igauge=0	igauge=1	igauge=0	igauge=1
0.8	0.795(3)	$0.781(2)\times10^{-32}$	0.0442(2)	$0.45(1)\times10^{-33}$
1.0	11.81(5)	$0.111(3)\times10^{-30}$	0.0585(2)	$0.59(1)\times10^{-33}$
1.2	86.5(4)	$0.44(1)\times10^{-29}$	0.1733(7)	$0.90(3)\times10^{-32}$

4. Running time and restrictions

The code generation for both processes considered in Table I takes a fraction of a second time. The MC computation with $10 \times 200\,000$ calls takes about 120 s and 40 s time for $\pi^+\pi^-\pi^+\pi^-\gamma$ and $\pi^+\pi^-\mu^+\mu^-\gamma$ final states on the processor Intel® Core™ i5-3470 CPU @ 3.20 GHz with a 64 bit Intel Fortran compiler.

As in previous versions of the program, the number of particles in the final state is limited to 10, which exceeds typical numbers of particles observed in the exclusive low energy e^+e^--annihilation processes. However, in the presence of photon–vector meson mixing, the Feynman diagrams proliferate, for example, with currently implemented Feynman rules, there are 90672 diagrams of the process $e^+e^- \to 3(\pi^+\pi^-)$. Thus, the compilation time of generated code may become very long already for processes with smaller than 10 a number of the final state particles.

REFERENCES

[1] S. Riemann, *Acta Phys. Pol. B* **46**, 2213 (2015), this issue.
[2] T. Lesiak, *Acta Phys. Pol. B* **46**, 2221 (2015), this issue.
[3] T. Riemann, *Acta Phys. Pol. B* **46**, 2235 (2015), this issue.
[4] G. Ecker, J. Gasser, A. Pich, E. de Rafael, *Nucl. Phys. B* **321**, 311 (1989).
[5] M. Bando, T. Kugo, K. Yamawaki, *Phys. Rep.* **164**, 217 (1988); M. Harada, K. Yamawaki, *Phys. Rep.* **381**, 1 (2003).
[6] K. Kołodziej, *Comput. Phys. Commun.* **180**, 1671 (2009).
[7] K. Kołodziej, *Comput. Phys. Commun.* **185**, 323 (2014).
[8] M. Benayoun, P. David, L. DelBuono, F. Jegerlehner, *Eur. Phys. J. C* **72**, 1848 (2012).
[9] K. Kołodziej, *Comput. Phys. Commun.* **196**, 563 (2015).
[10] S. Tracz, H. Czyż, *Acta Phys. Pol. B* **44**, 2281 (2013).